Off-axis Current Drive and Current Profile Control in JT-60U

T. Suzuki 1), S. Ide 1) , T. Fujita 1), T. Oikawa 1), M. Ishikawa 1), N. Hayashi 1), O. Naito 1), M.Sueoka 1), M. Seki 1), and the JT-60 Team

1) Japan Atomic Energy Agency, Naka, Ibaraki-ken, 311-0193 Japan

e-mail contact of main author: suzuki.takahiro@jaea.go.jp

Abstract. For the first time, we have measured the current density profile for off-axis neutral beam current drive (NBCD), using motional Stark effect (MSE) diagnostic. A spatially localized NBCD profile was clearly observed at ρ=0.6-0.8. The location was also confirmed by multi-chordal neutron emission profile measurement. The total amount of the driven current (0.15 MA) was consistent with the decrease in the surface loop voltage. The off-axis current drive can raise safety factor (q) in the center and help to avoid instability that limits performance of the plasma. We have developed a real-time control system of the minimum q (q_{min}), using the off-axis current drive. Injection power of lower-hybrid (LH) waves, and hence, its off-axis driven current controls q_{min}. In a high β plasma (β_N=1.7, β_p=1.5), the system was adopted to control q_{min}. With the control, q_{min} was raised and MHD fluctuations were suppressed. The stored energy increased by 16 % with the MHD fluctuations suppressed.

1. Introduction

Development of advanced scenario is required in realization of the future fusion reactor having high confinement and high stability in the core plasma. Actually, in the international thermonuclear experimental reactor (ITER), two advanced scenarios have been proposed, i.e. hybrid-operation and steady-state operation scenarios. Candidates for the scenarios can be either a positive shear plasma or reversed shear plasma, respectively. It is well known that the current profile in both the positive shear and reversed shear plasmas plays important roles in confinement and stability. Thus, optimization of current profile (or safety factor (q) profile) is essential in such advanced scenarios.

The optimization of current profile means control of current profile. In a long-pulse operation aiming at steady-state operation for fusion reactor, pre-programmed control of external current driver is not enough for current profile control. Current profile control in 'real-time' during the discharge is required. In 2004, JT-60U demonstrated the real-time control of current profile at low β in L-mode discharges. In such low β condition, plasma can be MHD stable and change in pressure, and hence bootstrap current is small. Driven current can be sufficient in low-density condition, in order to modify current. It is expected that the situation dramatically changes in a high β plasma. MHD instability affects pressure profile and bootstrap current. High-density condition reduces externally driven current. More importantly, in order to keep high β, such MHD instability should be avoided or stabilized through the optimizing current profile. Since external current drive power is limited due to some economic (reduction of circulating power in a plant) or technical reasons (equipment of current drivers), smaller control is better. Thus, JT-60U has proceeded to the real-time current profile control in a high β plasma. Since low q rational surface usually plays harmful role, minimum of the safety factor is controlled in order to eliminate the MHD resonant rational surface.

In the optimization of current profile, external current drivers must modify current profile, in combination with inherent inductive and bootstrap currents. There are two promising on-axis current drivers, neutral beam current drive (NBCD) and electron cyclotron current drive (ECCD). On-axis NBCD was already investigated in detail on JT-60U [1,2]. On-axis ECCD was also studied well in JT-60U [3,4] and in DIII-D [5,6]. On the other hand, off-axis current drivers would be lower-hybrid current drive (LHCD) or NBCD. Although it is difficult to drive current off-axis, where electron temperature, and hence, current drive efficiency is low, optimization of current profile needs a reliable off-axis current driver. Although LHCD was studied well in various devices including JT-60U [7,8], study on the off-axis NBCD is still under way. In the previous attempt to measure the off-axis NBCD profile in JT-60U, a low density condition to increase off-axis NB driven current j_{BD} made it difficult to calculate j_{BD} in conventional NBCD codes. Injection of EC waves to raise electron temperature for higher off-axis NBCD efficiency complicated the interpretation of change in current profile, since separation of EC driven current, bootstrap current and NBCD current was difficult. While in ASDEX-Upgrade [9], change in pitch angles of an MSE diagnostic induced by off-axis NBCD was compared to simulations. They found the change was smaller than the ASTRA simulation. Later, they reported that the change agrees with ASTRA/TRANSP simulation under a certain heating power or assumption of fast ion diffusion [10,11], but in some cases, the off-axis NBCD did not show change in pitch angles compared to on-axis NBCD [10,11]. Thus, understanding of the off-axis NBCD is tangled, in spite of increasing importance of the off-axis current drive on current profile control. We investigate off-axis NBCD again here using newly developed analysis technique [12] to evaluate small change in current profile from MSE and newly equipped neutron emission profile diagnostic [13].

Section 2 describes various current drivers in JT-60U. Using one of the neutral beams, off-axis NBCD is investigated in detail in section 3. Real-time control of current profile by LHCD in a high β plasma is demonstrated in section 4, simultaneously using the off-axis NBCD described in section 3.

2. Current drivers in JT-60U

JT-60U has 11 units of neutral beam injectors with positive ion source (P-NBI) and one unit of neutral beam injector based on negative ion source (N-NBI). Injection energies of the P-NBI and N-NBI are 80-85 keV and 300-400 keV, respectively. Injection powers of the P-NBI and N-NBI are 2-2.5 MW and 5-7 MW, respectively. Injection energy and power depends on pulse length of injection. P-NBI and N-NBI have two ion sources (A and B) in each unit. Figure 1 shows the poloidal cross section of JT-60U with NB trajectories. Two of 4 tangential P-NBIs are on-axis and the others are off-axis, in usual magnetic configuration in JT-60U. One of the two on-axis or two off-axis P-NBIs is injected to co-direction to the plasma current, and the others are to counter-direction for co/counter current drive, respectively. Seven P-NBIs are injected almost perpendicular to the plasma current. Four of the seven P-NBIs injected from upper outboard are for on-axis heating, and the other three P-NBIs injected from lower outboard are for off-axis heating. N-NBI is tangentially injected to co-direction to the plasma current. One of two beams from two N-NBI ion sources can be on-axis and another is slightly off-axis, in the usual configuration in JT-60U. Combination of these NBI systems enables us to realize various heating/current drive conditions, flexibly. LH antenna 'A' having multi-junction structure locates above

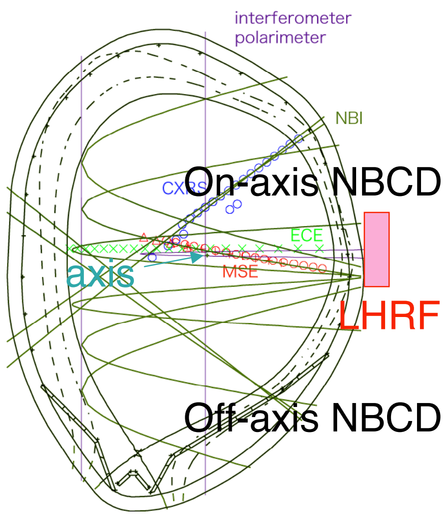

FIG. 1. Poloidal cross-section of the plasma and projection of trajectories of P-NB and N-NB.

equatorial plane. Power of LH waves can be controlled continuously up to 1.5 MW at every 10 ms, which gives advantage in controlling driven current. The other LHRF systems are not available. The parallel refractive index of primary component of the LH wave spectrum ranges 1.4-2.1, depending on phase difference of LH waves from two adjacent antenna modules. In order to obtain stable coupling of the LH waves, the gap between the plasma and the antenna front is controlled fixed during LHCD.

3. Measurement of off-axis NB driven current profile

The off-axis NBCD profile was measured in a plasma with ELMy H-mode at I_p=1.2 MA, B_t=3.8 T, and q_{95}=5.4. A tangentially line averaged electron density n_e=3.3x10^{19} m^{-3}. Figure 2 shows waveforms of the discharge. During the flat-top phase of plasma current, we injected about 2MW of the co-off-axis NB (t=7-12 s), with 7 MW of balanced on-axis diagnostic NBs. At this electron density, absorption of NB is sufficiently large, and slowing down time of beam ions (about 0.2 s) is much less than the off-axis co NBCD duration (5 s). Current was fully penetrated before off-axis NBCD. There was no MHD instability including sawtooth, except ELMs. Before and after the on-axis co NB injection, perpendicular off-axis NB of 2 MW was injected in order to compensate the total heating power (9 MW); see Fig. 2 (b). Figure 3 shows poloidal cross section of the plasma, optimized for tangential NB#10 to pass sufficiently off-axis. During most of the NB heating phase, the line averaged electron density and the diamagnetic stored energy (or the averaged pressure) are kept fixed (Fig. 2 (c) and (d)). Figure 4 (a) shows a contour plot of increment in current δI enclosed between adjacent MSE measurement points. The reference of the increment is the current profile at t=6.9 s (0.1 s before the start of the NBCD). A clear spatially localized increase in current has been observed at ρ=0.6-0.8 by application of the NBCD (t=7-12 s). In order to keep the Shafranov shift and the bootstrap current constant, 2 MW of perpendicular injection NB was injected before and after the off-axis NBCD. Thus, the off-axis NBCD mainly contributes to the change in current profile. Diffusion of the inductive electric field by the NBCD moved the location of current decrease inward from ρ=0.6 to ρ=0.35 during t=7-8 s. In about 1.5 s from the start of the NBCD, the local change in current profile has reached a steady state, where the resistive diffusion time was 1.6 s.

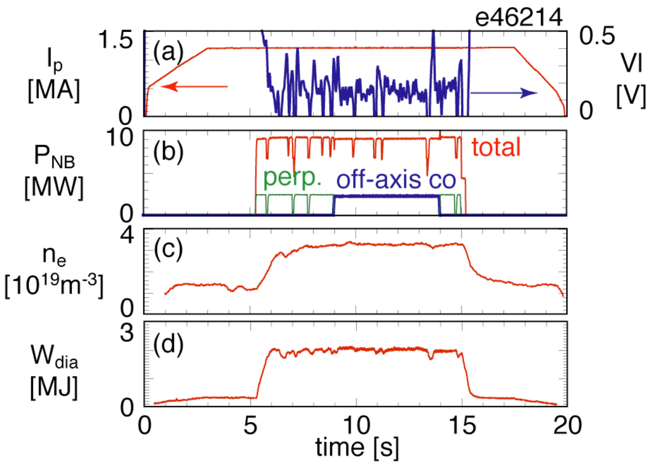

FIG. 2. Waveforms of discharge for off-axis NBCD profile measurement; (a) plasma current (red) and loop voltage (blue), (b) total NB power (red), off-axis co-NB power (blue), and perpendicular NB power that compensate PNB during stop of off-axis co NBCD, (c) a line averaged electron density, (d) diamagnetic stored energy.

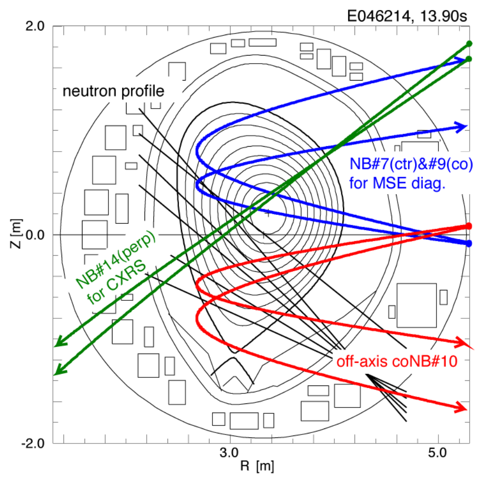

FIG. 3. Poloidal cross-section of the plasma and projection of trajectories of P-NB and N-NB. In order for NB#10 to pass enough off-axis, configuration was optimized. Sight lines of neutron emission profile measurement are drawn.

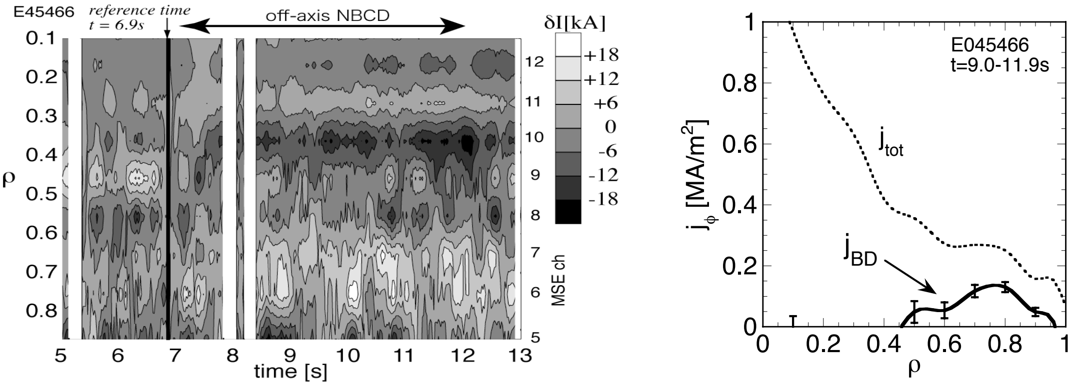

FIG. 4. (a) Temporal evolution of increment of current (kA unit) in case of the co-off-axis NBCD during t=7-12 s. Increase in current is indicated by light colors, while decrease by dark ones. Spatially localized increase in current was clearly observed at ρ=0.6-0.8. (b) Measured beam driven current density profile (solid curves) with total current density profile (dotted curves). The measured NBCD profile is spatially localized at off-axis, and its location is consistent with Fig.4 (a).

Loop-voltage profile analysis technique [14] using the MSE shows that toroidal electric field profile $E_\phi(\rho)$ is almost spatially uniform (within ±9 %). Subtracting Ohmic and bootstrap current profiles ($\sigma_\phi(\rho)E_\phi(\rho)$, $j_{BS,\phi}(\rho)$) from total current profile $j_{tot,\phi}(\rho)$ gives the beam driven current profile $j_{BD,\phi}(\rho)$ (Fig. 4 (b)). Here, we adopt neo-classical conductivity σ_ϕ. The peak of j_{BD} at ρ~0.75 in Fig. 4 (b) is consistent with the location of current increase in Fig. 4 (a). The driven current I_{BD} was 0.15 MA (CD efficiency 0.54×10^{19} AW^{-1}m^{-2}). Decrease in measured surface loop voltage during the NBCD also gives I_{BD}=0.16 MA.

Figure 5 shows chord-integrated neutron production rates [13] during and after the NBCD, as a function of the tangential minor radius ρ_{min}. The sight lines are shown in Fig. 3. Since estimated thermal ion contribution to neutron yield (th-th) is less than 1 %, the rate can be a measure of the number of beam ions. The result is consistent with Fig. 4 (b).

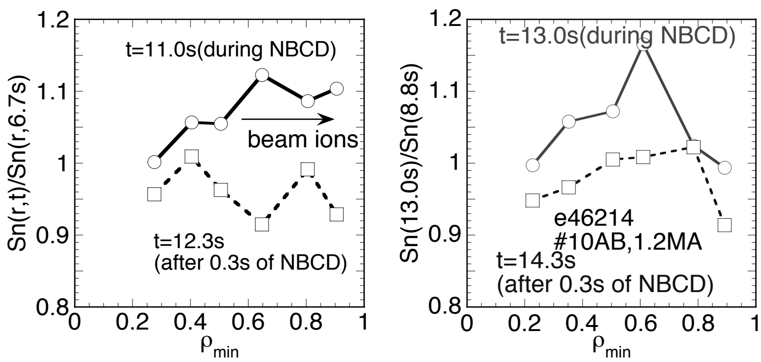

FIG. 5. Chord-integrated neutron production rate profile $S_n(\rho,t)$ during NBCD, and 0.3 s after NBCD for (a) I_p=0.8 MA and (b) I_p=1.2 MA. Beam ions produced by the NBCD is more spatially localized for higher I_p.

4. Control of current profile in a high β plasma using off-axis current drivers

Steady attainable β in JT-60U is usually limited by a neo-classical tearing mode (NTM), when rational surfaces having q=1.5 or 2 exist. The NTM can be stabilized when the minimum of safety factor (q_{min}) is raised above the corresponding values. In positive shear plasmas, increase in off-axis driven current raises q_{min}. Thus, we expect to stabilize the NTM, using the off-axis current drivers. While NBCD system in JT-60U does not have continuous controllability of injection power, LHCD system does. The LHCD is also a strong off-axis current driver [15]. Thus, we have constructed the real-time control system of q_{min} using the

LHCD. The safety factor profile is evaluated in real-time [16], at 9 spatial points of MSE diagnostic. In every time slices, q_{min} is calculated as quadratic minimum of 3 measurement points having smallest q. The system controls q_{min} to a given reference value ($q_{min,ref}$) through injection power of LH waves (P_{LH}), according to the following relation; $dP_{LH}/dt = -\alpha(q_{min}-q_{min,ref})$. The proportional gain α (positive value) determines response of the system. Parallel refractive index ($N_{//}$) that affect LHCD location was fixed in this q_{min} control.

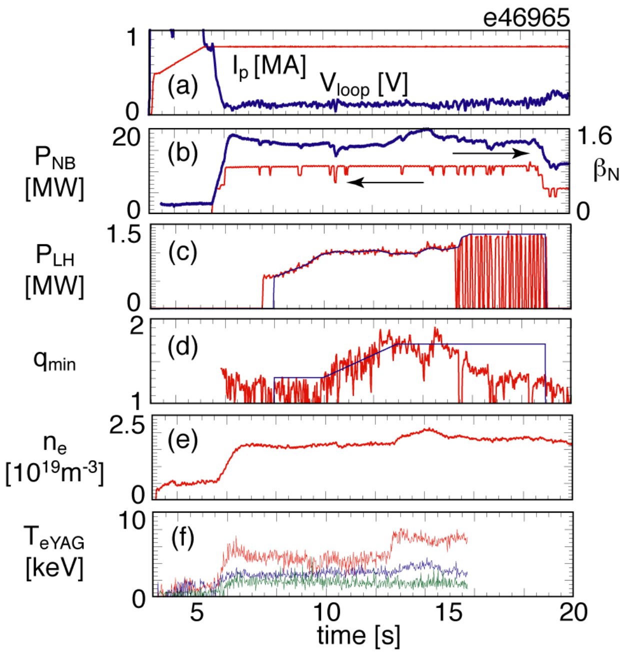

FIG. 6. Waveforms of the discharge for real-time q_{min} control. (a) plasma current (red) and loop voltage (blue), (b) neutral beam power (red) and normalized β (β_N, blue), (c) command LH power (blue) and injection power, (d) q_{min} calculated in real-time (red) and reference of q_{min} (blue), (e) a line averaged electron density, (f) electron temperatures at ρ = 0.17 (red), 0.37 (blue), 0.63 (green).

The real-time control of q_{min} was successfully demonstrated in a high β_p ELMy H-mode plasma (I_p=0.8 MA, B_t=2.5 T, q_{95}=5.9) shown in Fig. 6. During constant NB heating phase at 11 MW, LH waves was injected at 7.5 s, and real-time control of q_{min} started from t=8s. The initial LH power before the control (t=7.5-8 s) was preprogrammed at 0.55MW. LH waves are injected at fixed $\Delta\phi=30^o$ (primary $N_{//}\sim1.7$. The co-off-axis NBCD helped to raise q_{min} before the q_{min}-control above unity. The reference value of the q_{min} was set to 1.3 during t=8-10 s. During t=10-13 s, reference of q_{min} was proportionally increased from 1.3 to 1.7, and the $q_{min,ref}$ was kept constant. After the start of q_{min} control, q_{min} was about 1.1-1.2 and slightly lower than the $q_{min,ref}$=1.3. Thus q_{min} controller increased LH power gradually after t=8 s. Since the proportional gain α was 2 MWs^{-1} in this discharge, difference of q_{min} and $q_{min,ref}$ of 0.1 gives increasing rate in LH power of 0.2 MWs^{-1}. The minimum of q profile near the plasma center started increasing at t=9.5-10 s. Since the increasing rate of q_{min} during t=10-13 s was about the same as that of $q_{min,ref}$, the q_{min} controller stopped increasing LHCD power. At LH power of about 1 MW, q_{min} increased from 1.3 to 1.7, taking 3 seconds. LH power was properly controlled so as not for the q_{min} to overshoot its reference. During t=13-15 s, q_{min} was controlled to 1.7 until the start of the notching of the LH power at t=15.3 s. The notching was caused by interlock of LHRF system at arc detection in front of the antenna. Figure 7 shows the safety factor profiles before and during q_{min} control. The safety

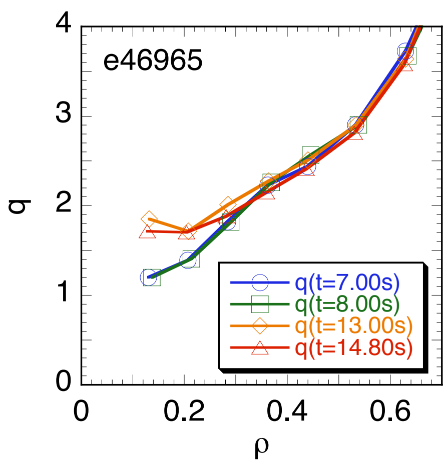

FIG. 7. Safety factor profiles; before LHCD (t=7.0 s, red), during LHCD and before control (t=8.0 s, green), during control (t=13.0 s, orange), during control and just before LH power notching (t=14.80 s, blue).

factor inside ρ=0.3 was clearly raised by the LHCD through the q_{min} control. After the notching of LH power, effective injection power was decreased, and LH driven current was not enough to sustain q_{min}=1.7 so that q_{min} gradually decreased down to 1.3. In this discharge, increase in β_N (from 1.3 to 1.6) was observed after t=12.5 s, when q_{min} was raised. Along with this increase in β_N, a line averaged electron density starts increasing and electron temperature also increased in the center of the plasma. Suppression of some instability might be a cause in the β_N increase, but this has not been clarified, yet for this discharge; see the last paragraph of this section.

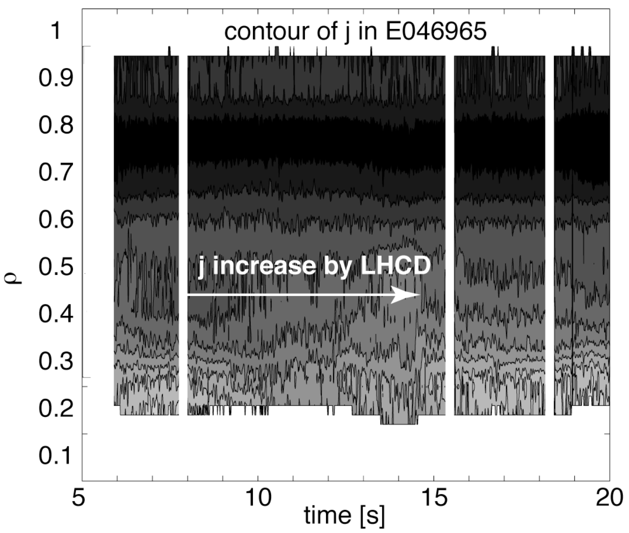

FIG. 8. Contour plot of current density profile j(ρ,t) at every 0.1 MAm^{-2} intervals. Lighter color indicates larger current density. After the start of LHCD at t=7.5 s, j at ρ=0.3-0.5 gradually increases, showing that LH waves driving current at this location. Change in current profile outside ρ=0.6 is small.

Although q_{min} does not significantly change during t=8-10 s, current profile (or q profile) inside ρ=0.5 is changing due to the application of LHCD. Figure 8 shows a contour plot of the current density profile j(ρ,t). From t=7.5-10 s, current density at ρ=0.2 is decreasing so that q is increasing. In Fig. 8, we can also see current density increases at ρ =0.3-0.5, after application of LHCD and q_{min} control. Current density outside ρ =0.6 is small. This increase is a result of spatially localized LHCD at this location (ρ=0.3-0.5). Spatial diffusion of inductive electric field (so called, back EMF) brought decrease in current density inside ρ=0.2, and increase in q_{min}. Increase in current density at t=13-15 s at ρ =0.2 would be caused by decrease in electric resistivity due to increase in central electron temperature as seen in Fig. 6 (f). The electron temperature comes from improvement in confinement by the q_{min} control. Thus, the current profile and temperature (or pressure) profiles are interacting each other in a complex manner. In such a plasma, q_{min} was controlled, here.

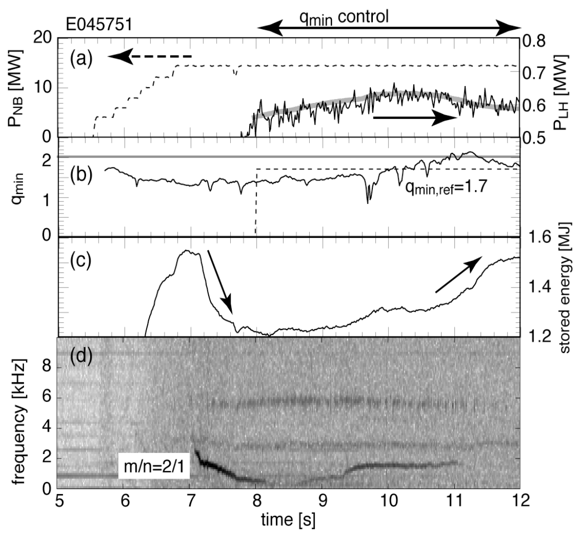

FIG. 9. (a) NB injection power (dotted), LH injection power (thin solid), and its command value (thick solid). (b) q_{min} (solid) and its reference (dotted, $q_{min,ref}$=1.7). Gray line indicates q_{min}=2. (c) stored energy. (d) contour map of spectrum of magnetic fluctuations. The control of q_{min} started from t=8 s.

Figure 9 shows waveforms of the discharge where MHD stability was clearly suppressed by the q_{min} control. In order to produce high β_p-mode plasma, 14 MW of NBs (including co-off-axis NB) were injected into a plasma having I_p=0.8 MA, B_t=2.4 T during the flattop phase of I_p. When stored energy W_{dia} reached 1.55 MJ (β_N=1.7, β_p=1.5), the m/n=2/1 NTM appeared, leading to decrease of W_{dia} by 22 %. LH waves were injected from t=7.5 s. Control of q_{min} by P_{LH} started at t=8 s, at fixed $\Delta\phi=0^o$ (primary $N_{//}$~1.65). We set $q_{min,ref}$=1.7 to eliminate q=1.5 rational surface in the plasma. When the q_{min} control started, P_{LH} increased to raise q_{min}. The q_{min} reached to 1.7 and the LH power decreased by the control. The q_{min} overshot the $q_{min,ref}$, and reached to 2 at t~11 s. The overshoot in q_{min} was caused by insufficient adjustment of the proportional gain α=0.3 MWs^{-1}. At this time, fluctuation at 1.6 kHz was stabilized, and W_{dia} started increasing back to the initial value. Due to the reduction of LH power from t~10 s, q_{min} decreased down to $q_{min,ref}$=1.7 at t~12 s.

5. Summary

We have measured the current density profile for off-axis neutral beam current drive (NBCD), using motional Stark effect (MSE) diagnostic. A spatially localized NBCD profile was clearly observed at ρ=0.6-0.8. The location was also confirmed by multi-chordal neutron emission profile measurement. The total amount of the driven current (0.15MA) was consistent with the decrease in the surface loop voltage. The off-axis current drive can raise safety factor (q) in the center and help to avoid instability that limits performance of the plasma. We have developed a real-time control system of the minimum q (q_{min}), using the off-axis current drive. Injection power of lower-hybrid waves, and hence, its off-axis driven current controls q_{min}. In a high β plasma (β_N=1.7, β_p=1.5), the system was adopted to control q_{min}. With the control, q_{min} was raised and MHD fluctuations were suppressed. The stored energy increased by 16 % with the MHD fluctuations suppressed.

The authors thank to the JT-60 team for cooperation in conducting this experiment. This work was partially supported by Grand-in-Aid for Young Scientists (B) No. 18760650 and Grand-in-Aid for Scientific Research No. 18560798 and 16082209 from MEXT.

References

[1] OIKAWA, T., et al., Nucl. Fusion **40** (2000) 435.
[2] OIKAWA, T., et al., Nucl. Fusion **41** (2001) 1575.
[3] SUZUKI, T., et al., Plasma Phys. Control. Fusion **44** (2001) 1.
[4] SUZUKI, T., et al., J. Plasma Fusion Res. **80** (2004) 511.
[5] PETTY, C.C., et al., Nucl. Fusion **42** (2002) 1366.
[6] PETTY, C.C., et al., Nucl. Fusion **43** (2003) 700.
[7] IDE, S., et al., Phys. Rev. Lett. **73** (1994) 2312.
[8] NAITO, O., et al., Phys. Rev. Lett. **89** (2002) 065001.
[9] HOBIRK, J., et al., 30th EPS Conference (2003) O-4.1B.
[10] GUENTER, S., et al., 31st EPS Conference (2004) O-1.02.
[11] GUENTER, S., et al., 32nd EPS Conference (2005) P-4.075.
[12] SUZUKI, T., et al., J. Plasma Fusion Res. **80** (2004) 362.
[13] ISHIKAWA, M., et al., Rev. Sci. Instrum. **73** (2002) 4237.
[14] FOREST, C.B., et al., Phys. Rev. Lett., **73** (1994) 2444.
[15] IDE, S., et al., Plasma Phys. Control. Fusion **44** (2002) L63.
[16] SUZUKI, T., et al., Proceeding of 20th IAEA Conference (2004) IAEA-CN-116/EX/1-3.